



Risk analysis of energy efficiency investments in buildings using the Monte Carlo method

Eisuke Togashi

To cite this article: Eisuke Togashi (2018): Risk analysis of energy efficiency investments in buildings using the Monte Carlo method, Journal of Building Performance Simulation, DOI: [10.1080/19401493.2018.1523949](https://doi.org/10.1080/19401493.2018.1523949)

To link to this article: <https://doi.org/10.1080/19401493.2018.1523949>



Published online: 27 Sep 2018.



Submit your article to this journal [↗](#)



View Crossmark data [↗](#)

Risk analysis of energy efficiency investments in buildings using the Monte Carlo method

Eisuke Togashi*

Department of Architecture, Kogakuin University, Shinjuku-ku, Japan

(Received 23 June 2018; accepted 11 September 2018)

Demonstrating the economic rationality of investments in energy efficiency is a necessary step in reducing the energy consumption of buildings. Generally, financial instruments are evaluated according to both the return on investment and the risk. However, many previous studies of energy efficiency investments in buildings are based on deterministic scenarios and do not evaluate the risk levels of these investments. Therefore, in this study, we clarify the risk involved in an energy-saving investment by calculating the probability distribution of the energy reduction and evaluating the result using financial engineering methods. We first develop a stochastic model of various conditions that affect the energy consumption of a building. These conditions include weather processes, office worker behavior, tenant characteristics, and tenant replacements. Next, we construct a prediction model of a building's energy consumption, and we use our stochastic model to create the boundary conditions of this prediction model. By repeatedly performing energy consumption predictions using the Monte Carlo method, we can obtain the probability distribution for building energy consumption. Finally, given this probability distribution, we evaluate energy efficiency investments using financial engineering methods. Based on the discounted cash flow distribution, we calculate the risk premium of each energy efficiency investment, and, based on the variance and covariance matrix of the internal rate of return of each energy efficiency investment, we find the optimal investment ratio.

Keywords: risk analysis; energy efficiency investment; Monte Carlo method; HVAC; portfolio theory

1. Introduction

The household and services sectors, both of which are related to buildings, contribute about 40% of the world's total final energy consumption (International Energy Agency 2008). Thus, improving the energy efficiency of buildings has the potential to greatly contribute to the reduction of world energy consumption. Making such improvements, however, requires investments, and investors will only make these investments if they improve the value of real estate. There are three traditional approaches to real estate valuation: the "sales comparison approach," the "income approach," and the "cost approach" (Appraisal Institute 2013; MLIT 2014). Therefore, it is quite natural to use these approaches when considering the influence of energy efficient investments on real estate value. Yamagata et al. (2011) review international studies of the effect of green building on office rents or housing prices and report that these studies can be categorized as validating one of two hypotheses. The first hypothesis is that market participants prefer real estate with sustainability. These studies focus on how green buildings are traded by market participants and are closely related to the sales comparison approach to real estate appraisal. The second hypothesis is that expectations of reduced energy consumption are reflected in real estate

prices. These studies aim to clarify the effect of energy conservation on real estate income streams and are closely related to the income approach.

Several researchers use a sales comparison approach to examine whether the benefits of energy efficiency improvements to buildings are worth the cost of investment. Some investigate the relationship between environmental certification and real estate prices (Chegut, Eichholtz, and Kok 2014; Eichholtz, Kok, and Quigley 2010, 2013; Fuerst and McAllister 2011a, 2011b; Miller, Spivey, and Florance 2008; Wiley, Benefield, and Johnson 2010). Eichholtz, Kok, and Quigley (2010, 2013) analyze the influence of Leadership in Environmental Energy and Design (LEED) and Energy Star labeling using a dataset of rented (21,000 cases) and sold (6000 cases) buildings in the US marketplace. Based on hedonic analysis, they show that an office building registered with LEED or Energy Star rents for a 3% premium on average and sells for a premium of about 13%. Fuerst and McAllister (2011a, 2011b), Miller, Spivey, and Florance (2008), Wiley, Benefield, and Johnson (2010), and Chegut, Eichholtz, and Kok (2014) also analyze properties traded on the market in a similar way and quantify the impacts of LEED, Energy Star, and the Building Research Establishment Environmental Assessment Method on rents and sales prices. These studies use a

*Email: e.togashi@gmail.com

social scientific approach, which is helpful for understanding actual changes in societal preferences.

On the other hand, there is a known gap between the investment expected based on the theoretical profit improvement rate reported by various studies and the energy-saving investment actually observed in the market, which is called the “efficiency gap” (see Gillingham and Palmer (2014) for a comprehensive review). In other words, investors tend to prefer lower initial investments over higher monthly rental revenues, and internal investment rates are often set at levels higher than the cost of capital. Research has examined the cause of this “efficiency gap,” and some studies argue that the energy-saving investment market is imperfect (DeCanio 1993; Sanstad and Howarth 1994; Schleich 2009).

Specifically, DeCanio (1993) argues that energy-saving investment faces a principal-agent problem. In many corporations, managers tend to be rotated through different jobs every few years. They prefer projects with short payback periods, even if the projects are inferior to energy-saving investments in the long term, because the quick returns on such projects enhance these managers’ reputations. Sanstad and Howarth (1994) and Schleich (2009) argue that imperfect or asymmetric information causes market failures. For example, the measurement level of a current facility may be insufficient, and many corporations do not know how much energy their facilities are consuming or current energy consumption patterns. Moreover, these corporations may be unfamiliar with the latest energy efficiency investments available and may not know the current energy consumption levels of other facilities. Sanstad and Howarth (1994) and Schleich (2009) also point out that hidden costs cause market failures. In other words, they argue that corporations do not make energy efficiency investments because these investments have additional costs that are hidden to observers but not to corporations, such as the cost of obtaining information to determine whether to make an energy efficiency investment, the cost of an inferior indoor environment, the cost required for maintaining energy efficient equipment, and so on.

The risk of future uncertainty is one of the main causes of market failure that may explain the “efficiency gap.” This study aims to quantitatively evaluate this risk. Many previous studies have also focused on this risk (Abadie, Chamorro, and González-Eguino 2013; Ansar and Sparks 2009; Cano et al. 2014; Cano, Moguerza, and Alonso-Ayuso 2016; Jackson 2008, 2010; Szumilo and Fuerst 2017; Tuominen and Seppänen 2017). Szumilo and Fuerst (2017) argue that introducing sustainability to a real property offers two types of benefits to its financial performance. The first benefit is the direct financial benefit due to reduced utility costs, which should not attract additional risk. The second is the uncertain benefit of evoking additional tenant demand. It is uncertain whether this benefit is obtained, as tenants’ attraction to sustainability at the

time of signing the lease is stochastic. Empirical tests performed on a large panel dataset from the US show that energy efficient properties attract higher demand but that this demand depends on market conditions, increasing exposure to market risk.

Jackson (2008, 2010) points out that traditional methods of evaluating energy efficiency investments, such as requiring low paybacks or high internal rates of return (IRR), tend to exclude many profitable investments. This issue arises because the aim of these methods is risk avoidance rather than risk management. Jackson (2008) proposed the concept of the energy budget at risk (EBaR) to apply investment analysis to energy-related decisions in a manner that is consistent with financial investment analysis. EBaR is a risk management tool similar to value at risk, which is the most widely recognized such tool in the finance industry. It attempts to quantify the result of an energy efficiency investment as a probability distribution to provide information on the return from investment with the level of uncertainty.

Tuominen and Seppänen (2017) discuss the risk of unexpected utility cost hikes. Their study presents a method for calculating the value of the utility cost risk reduction to a consumer that can be achieved through energy efficiency investments. The value of reducing the utility cost risk is evaluated using a variation of the Black–Scholes model. Tuominen and Seppänen (2017) argue that this often-overlooked benefit of energy efficiency investments merits more consideration in future studies.

Cano et al. (2014) and Cano, Moguerza, and Alonso-Ayuso (2016) study the decision making processes for energy efficiency investments in buildings that are affected by uncertainties. Their study introduces a scenario tree model to represent various stochastic events and the investment decisions (installation, expansion, and renovation) for the events. By repeating the calculation with stochastically fluctuating utility costs, the distribution of investment costs is generated.

In reality, various kinds of energy efficiency equipment exist in buildings, and they exhibit different stochastic trends. For a big business decision, it is sufficient to calculate the total probabilistic trend of energy efficiency investments caused by combining various types of energy efficiency equipment. For this reason, all of the studies of risk described above consider the probabilistic trend of energy efficiency investment for an entire building and do not calculate the behavior of individual energy-saving equipment. However, in the design phase, when it is necessary to consider individual pieces of energy efficiency equipment, such risk assessments are too simple. It is necessary to understand the stochastic energy efficiency trend for each piece of equipment rather than for the entire building. Doing so helps to determine whether or not to introduce individual pieces of energy efficiency equipment, and, if many pieces of energy efficiency equipment are to be introduced, we can decide which one to prioritize.

Therefore, in this study, the uncertainty of energy efficiency investment efficacy is not expressed as a single simple probability distribution but is calculated based on a detailed physical model incorporating the Monte Carlo method. Then, based on the probabilistic trends for individual pieces of energy efficiency equipment, we use financial engineering methods to estimate the risk premium and solve the optimal investment allocation problem.

The remainder of this paper is structured as follows. In section 2, “Development of stochastic energy consumption prediction model,” various conditions that affect a building’s energy consumption are expressed as stochastic models. Specifically, we introduce stochastic models for weather processes, office worker behavior, tenant characteristics, and tenant replacements. Then, in section 3, “Stochastic energy consumption predictions,” we construct a prediction model of a building’s energy consumption. The probabilistic model developed in section 2 is used to create the boundary conditions of this energy consumption prediction model. By repeatedly calculating the predicted energy consumption using the Monte Carlo method, we obtain a probability distribution of a building’s energy consumption. In section 4, “Evaluation with financial engineering methods,” we use the probability distribution obtained in section 3 to evaluate energy efficiency investments according to financial engineering methods. We calculate the risk premium of each energy efficiency investment using the distribution of the discounted cash flow (DCF), and we determine the optimal investment ratio based on the variance and covariance matrix of the IRR of each energy efficiency investment. Finally, section 5, “Conclusions,” provides a discussion of the results, and concludes the paper.

2. Development of stochastic energy consumption prediction model

In this section, we introduce stochastic models of weather processes, office worker behavior, office tenant characteristics, and tenant replacements. These models will be integrated into a building energy simulation model in later sections.

2.1. Stochastic model of weather processes

This model was first developed by Yoshida (1992), and some improvements to express the influence of the cloud cover ratio were added by Togashi (2015). See Togashi (2015) for more details about this model as well as specific parameters for each expression. The weather conditions generated by this model are the dry-bulb temperature, absolute humidity, and atmospheric transmissivity. The amount of solar radiation is estimated based on the atmospheric transmissivity (Watanabe, Urano, and Hayashi 1983). In this model, as shown in Equation (1), each

weather condition at time n is expressed by four components: the trend T , the annual cycle CA , the circadian cycle CC , and an irregular component I .

$$Y_n = T_n + CA_n + CC_n + I_n \quad (1)$$

The trend component T_n can be used to express a long-term trend, such as the effect of global warming, but the long-term trend is assumed to be zero in this study. CA_n and CC_n are periodic components, both of which are represented by a Fourier series, as shown in Equation (2).

$$C_n = \frac{A_0}{2} + \sum_{i=1}^N \left[A_i \cos\left(\frac{2\pi in}{T}\right) + B_i \sin\left(\frac{2\pi in}{T}\right) \right] \quad (2)$$

Since atmospheric transmissivity is greatly affected by the amount of clouds, we create separate models for sunny and cloudy weather. Whether the weather is sunny or cloudy is modeled as a Markov process, as shown in Equations (3) and (4).

$$\begin{bmatrix} P_{F,t+1} \\ P_{C,t+1} \end{bmatrix} = \begin{bmatrix} P_{FF} & 1 - P_{CC} \\ 1 - P_{FF} & P_{CC} \end{bmatrix} \begin{bmatrix} P_{F,t} \\ P_{C,t} \end{bmatrix} \quad (3)$$

$$P_{\infty,C} = (1 - P_{FF}) / (2 - P_{CC} - P_{FF}) \quad (4)$$

P is the transition probability, and P_{∞} is the invariant distribution. Equation (2) includes a total of four sets of parameters A and B (i.e. parameters for the dry-bulb temperature, the relative humidity, and atmospheric transmissivity in the cases of sunny and cloudy weather).

The irregular component I_n is represented by an autoregressive model, as shown in Equations (5) to (7).

$$I_{ATn} = \sum_{i=1}^p a_{ATi} I_{ATn-i} + N(0, \sigma_{AT}) \quad (5)$$

$$I_{DTn} = \sum_{i=1}^p (a_{DTi} I_{DTn-i} + b_{DTi} I_{HRn-i}) + N(0, \sigma_{DT}) \quad (6)$$

$$I_{HRn} = \sum_{i=1}^p (a_{HRi} I_{DTn-i} + b_{HRi} I_{HRn-i}) + N(0, \sigma_{HR}) \quad (7)$$

The suffixes DT , HR , and AT represent the dry-bulb temperature, absolute humidity, and atmospheric transmissivity, respectively. $N(0, \sigma)$ is white noise with an average of zero and variance σ^2 . Since the dry-bulb temperature and the humidity ratio have mutual influences, a vector autoregressive model is used, as shown in Equations (6) and (7).

The periodic components (CA and CC) of the dry-bulb temperature and absolute humidity are corrected by irregular components of atmospheric transmissivity, as shown in

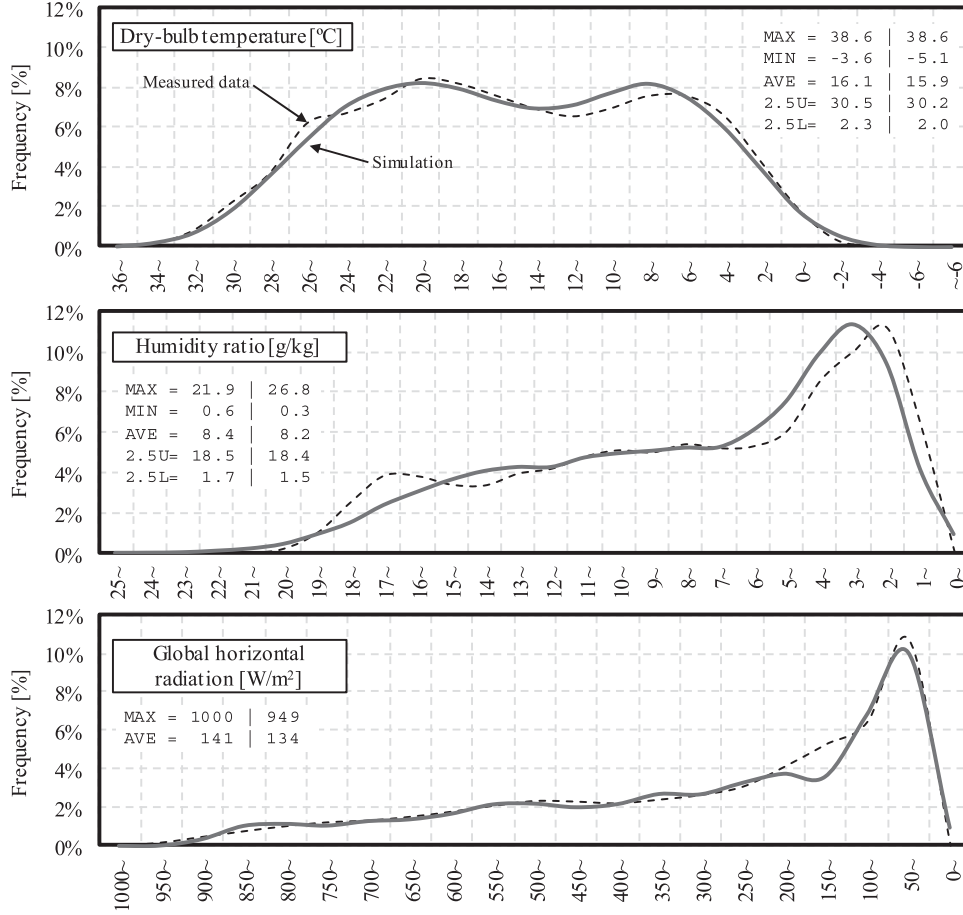


Figure 1. Frequency distribution of the calculated values of the model and the measured values (20 years).

Equations (8) to (10). The cf_x are correction coefficients.

$$CA_{cr} = CA \times (cf_{sh} \cdot I_{ATcr}) \quad (8)$$

$$CC_{cr} = CC \times (cf_{swA} \cdot I_{ATcr} + cf_{swB}) \quad (9)$$

$$I_{ATcr} = I_{AT} + CC_{AT} - (P_{\infty,F} CC_{ATF} + P_{\infty,F} CC_{ATC}) \quad (10)$$

The calculations in this study use parameters from Tokyo. Figure 1 shows that the frequency distribution of the values calculated by the model and that of values measured over twenty years total are well matched. Figure 2 shows an example of an annual weather simulation result.

2.2. Stochastic model of office worker behavior

Occupant behavior has a great influence on the energy consumption of a building. Gaetani, Hoes, and Hensen (2016) compare various occupant behavior models and conclude that determining the best complexity for occupant behavior modeling is strongly case specific. The model used in this study was developed based on a questionnaire survey of 1000 office workers in Japan. We provide a brief description of the model here, but for more details

about this model as well as specific parameters for each expression, see Togashi (2017). The model consists of four small stochastic models to reproduce the daily activities of office workers. The four probabilistic events are “time of attendance, lunch break, and leaving work,” “nightly work,” “holiday work,” and “other temporary leave.” The parameters of the model are estimated by gender (male and female), age (divided into five age groups from 20s to 60s), and job type and form of employment (general employees, managerial staff, executive officers, civil servants, and temporary contract employees).

In order to express the time of attendance, lunch break, and leaving work, the difference between the fixed time and the actual time, which includes overtime, is modeled. The “fixed time” mentioned here is the standard arrival or leaving time contracted between the employer and the employee. Many Japanese workers tend to arrive earlier than the fixed time and leave the company later than the fixed time. Therefore, the probability distribution of the difference between the fixed time and the actual time is not symmetrical. For this reason, Johnson’s SU (Equation (11)) and SB (Equation (12)) distributions, which are probability distributions with adjustable skewness, are introduced

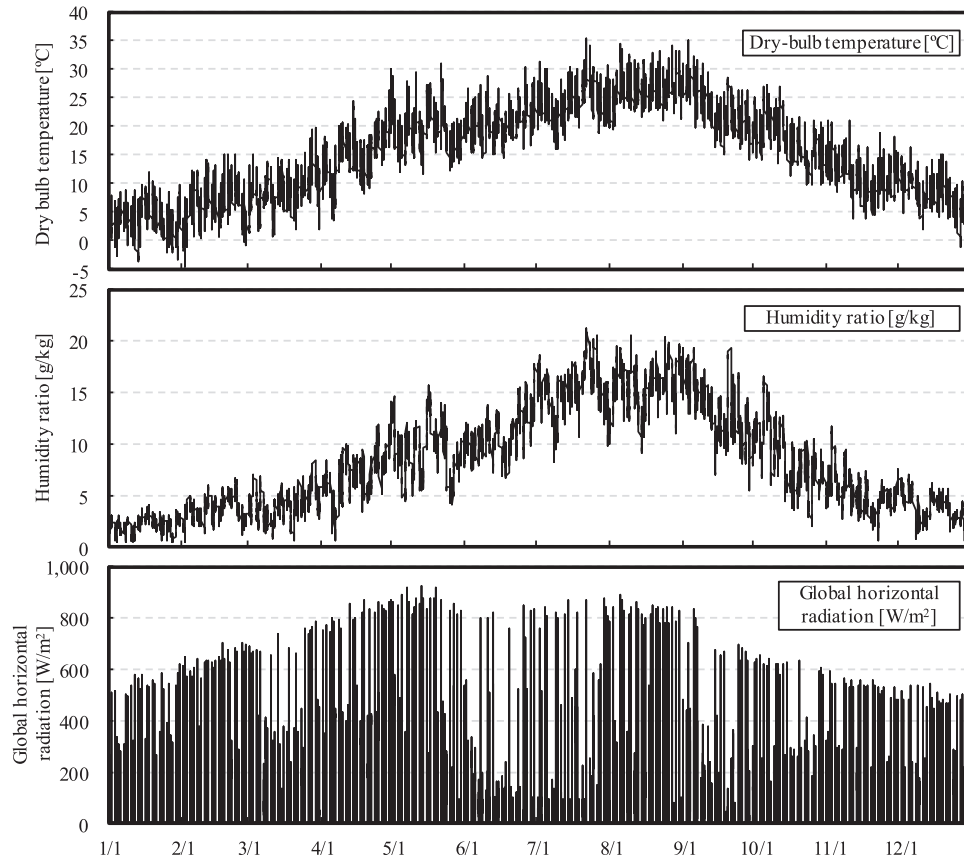


Fig. 2 Example annual weather simulation results for Tokyo

Figure 2. Example annual weather simulation results for Tokyo.

in this model.

$$P_{SU}(x) = \frac{\delta \exp \left[-0.5 \left\{ \gamma + \delta \ln \left(\frac{x-a}{b} + \sqrt{\left(\frac{x-a}{b} \right)^2 + 1} \right) \right\}^2 \right]}{\sqrt{2\pi} \sqrt{(x-a)^2 + b^2}} \quad (11)$$

$$P_{SB}(x) = \frac{\delta(b-a) \exp \left[-0.5 \left\{ \gamma + \delta \ln \left(\frac{x-a}{b-x} \right) \right\}^2 \right]}{\sqrt{2\pi} (x-a)(b-x)} \quad (12)$$

Figure 3 shows an example time difference distribution calculated using a Johnson distribution, which demonstrates the trend of early morning arrivals and overtime work. However, this example shows the overall average, and the distribution changes slightly according to age and gender.

Our model of nightly work recognizes that some office workers may work all night and some may never work at night. Based on the results of the questionnaire, the fraction of workers who work overnight can be estimated according to the job type and form of employment. For example, 21.5% of managerial staff are likely to work overnight,

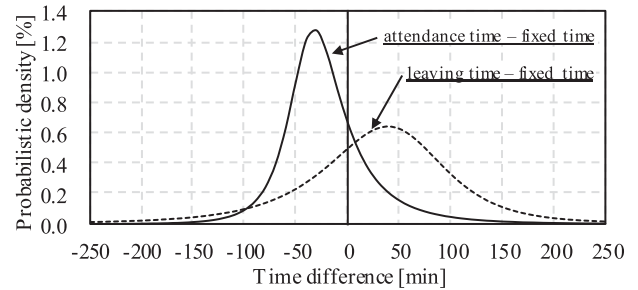


Figure 3. Probabilistic density of the time difference based on the Johnson distribution (weekday).

compared to only 4.5% of temporary contract employees. Office workers who have the potential to work all night are expected to do so with a probability of 1.2%.

The model of holiday work was created in the same way as that of night work. First, office workers who are likely to work on holidays are identified according to job type and form of employment. Then, from these workers, we identify the workers who work on holiday with a certain probability. We then model the arrival and leaving times for holiday workers using the Johnson distribution, as described above. Figure 4 shows the probabilistic density

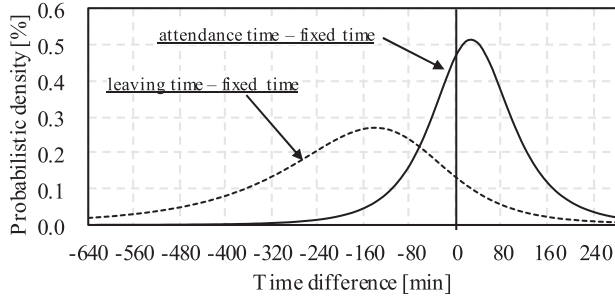


Figure 4. Probabilistic density of the time difference based on the Johnson distribution (holiday).

of this time difference based on a Johnson distribution. On holidays, workers tend to go to work later and leave work earlier than on weekdays.

Other temporary leave is modeled by the Markov chain shown in Equation (13). P_I is the probability of being indoors, and P_O is the probability of being outdoors.

$$\begin{bmatrix} P_{I,t+1} \\ P_{O,t+1} \end{bmatrix} = \begin{bmatrix} P_{II} & 1 - P_{OI} \\ 1 - P_{IO} & P_{OO} \end{bmatrix} \begin{bmatrix} P_{I,t} \\ P_{O,t} \end{bmatrix} \quad (13)$$

By integrating the above four stochastic models, the daily behavior of office workers can be calculated. Figure 5 shows an example calculation of the percentage of office workers who are indoors at each time of day. The long-term averages converge to the bold lines, but the specific day-by-day results differ, as indicated by the thin lines. Figure 6 shows an example calculation of the probability distribution of the difference between the fixed time (leaving) and the last exit time according to the size (number of office workers) of the tenant. If the number of office workers is large, there is a high probability that some office workers will stay at work late. Therefore, the distribution shifts to the right. Such a shift is important for energy efficiency analysis because it greatly affects the operation of the heating, ventilation, and air conditioning (HVAC) system.

2.3. Stochastic model of office tenant characteristics

As mentioned in the previous section, the parameters that affect the behavior of office workers differ according to job

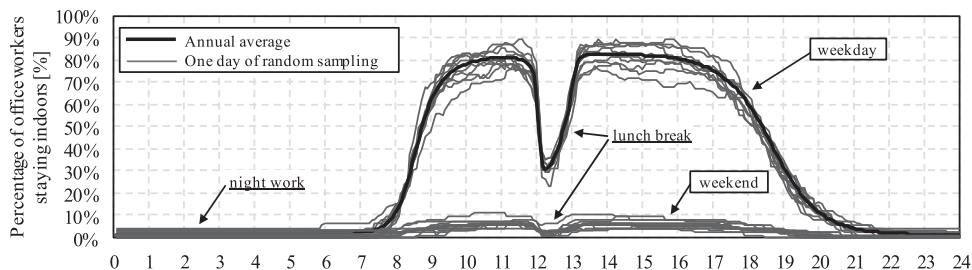


Figure 5. Percentage of office workers staying indoors by time of day.

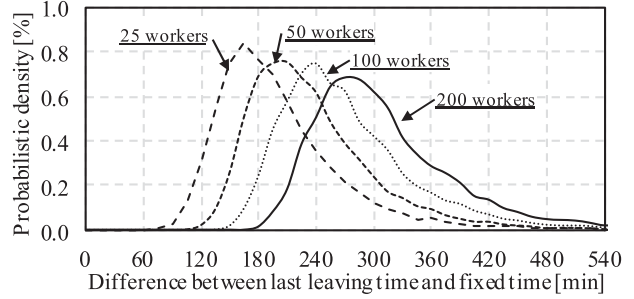


Figure 6. Probabilistic density of the difference between the last leaving time and fixed time.

type, form of employment, gender, and age. The composition ratio of the office workers, which incorporates factors such as gender and age, varies depending on the industry type of the tenant. Therefore, a stochastic model that estimates this composition ratio for the industry of a building's tenant is required.

For this model, we leverage data from the Statistics Bureau in Japan (SBJ). The SBJ conducts statistical surveys about the labor force every month to elucidate the current state of employment and unemployment in Japan (SBJ 2015). These surveys are summarized and published as the “Labor Force Survey.” By processing the results of these surveys, we can obtain the employment ratio by industry, gender, age, employment status, type of employment, and occupation, as shown in Tables 1 and 2 (Togashi 2018a). We can then generate the proportions of office workers by age, gender, and so on as discrete distributions based on the tenant's industry. The occupied desk area and the probability of an office worker staying in the room differ depending on the type of job. In this study, we assume that these values follow normal distributions. Using the survey results of Fujii et al. (1980), we can estimate the parameters, as shown in Table 3.

2.4. Stochastic model of tenant replacement

The model that we use for tenant replacement was originally developed by Kariya et al. (2005) for the evaluation of real options. The model expresses two probabilistic events: the risk of cancellation before the expiration of the

Table 1. Employment ratio [%] by industry, gender, employment status, and type of employment and occupation.

Industry	Gender	Administrative and managerial workers	Professional and engineering workers		Clerical workers		Sales workers	
			Regular employee	Part-time worker	Regular employee	Part-time worker	Regular employee	Part-time worker
Construction	male	18.5	27.0	5.6	18.0	3.7	22.5	4.7
	female	3.0	2.2	0.8	66.9	24.1	2.2	0.8
Manufacturing	male	11.9	27.0	5.7	30.0	6.3	15.8	3.3
	female	2.0	4.3	4.6	41.1	44.1	1.9	2.0
Electricity, gas, heat supply, and water	male	0.0	21.2	1.8	63.8	5.5	7.1	0.6
	female	0.0	0.0	0.0	75.0	25.0	0.0	0.0
Information and communications	male	2.7	61.5	7.2	16.6	2.0	9.0	1.0
	female	0.0	26.6	14.9	34.0	18.9	3.6	2.0
Transport and postal activities	male	10.5	2.6	0.9	56.6	18.9	7.9	2.6
	female	3.3	0.0	0.0	30.6	66.1	0.0	0.0
Wholesale and retail trade	male	11.5	4.8	1.6	19.7	6.6	41.8	14.0
	female	2.5	3.0	6.3	26.0	55.4	2.2	4.6
Finance and insurance	male	7.2	3.9	0.4	47.3	5.0	32.8	3.4
	female	0.0	0.8	0.4	44.1	24.2	19.7	10.8
Real estate and goods rental and leasing	male	14.9	1.5	0.6	36.7	14.3	23.0	9.0
	female	6.1	0.0	0.0	50.9	33.9	5.5	3.6

Table 2. Employment ratio [%] by industry and age.

Industry	Age				
	~ 29	30 ~ 39	40 ~ 49	50 ~ 59	60 ~
Construction	19.4	36.9	55.3	40.3	48.1
Manufacturing	30.3	42.3	54.5	41.7	31.2
Electricity, gas, heat supply, and water	12.5	50.0	95.8	29.2	12.5
Information and communications	43.5	60.8	57.2	29.1	9.4
Transport and postal activities	23.9	39.4	59.9	44.7	32.1
Wholesale and retail trade	37.8	39.1	47.6	37.8	37.7
Finance and insurance	32.6	36.4	59.1	49.1	22.8
Real estate and goods rental and leasing	24.3	34.2	40.5	35.5	65.5

Table 3. Parameters of probability distribution of “occupied area” and “percent staying indoors”.

Status or type of employment	Occupied area [worker/m ²]		Percent staying indoors [-]	
	μ	σ	μ	σ
Administrative and managerial workers and clerical workers	0.162	0.055	0.694	0.115
Sales workers	0.193	0.059	0.477	0.052
Professional and engineering workers	0.149	0.053	0.647	0.122

rental period and the risk of the time required to search for the next tenant after cancellation occurs.

To estimate the risk of cancellation, we assume that one contract period is 24 months based on Japanese laws and business practices. A tenant can cancel without a penalty if the lender is notified six months before the contract term expires. If there is no notice, the lease contract is automatically extended. Equation (14) expresses the probability that a tenant will cancel a lease contract in the m th month. In this model, we assume that no tenants cancel

with penalty.

$$p_{anc}(m) = \begin{cases} q_{anc}^{19-m} & (m = 1, \dots, 18) \\ 0 & (m = 19, \dots, 24) \end{cases} \quad (14)$$

The number of months required to search for a new tenant is represented by a negative binomial distribution, as shown in Equation (15). Assuming that μ_{sek} and σ_{sek} are the average and variance of the number of months required to search for a new tenant, the parameters q_{sek} and

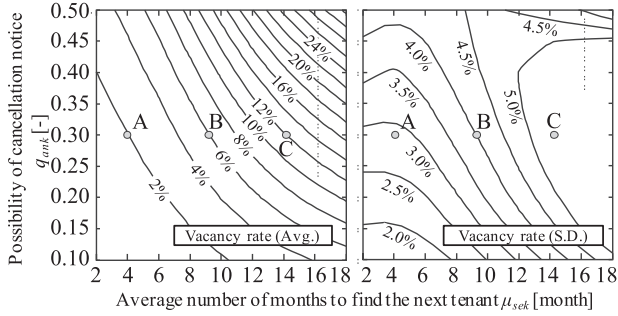


Figure 7. Average and standard deviation of the vacancy rate for values of μ_{sek} and q_{sek} .

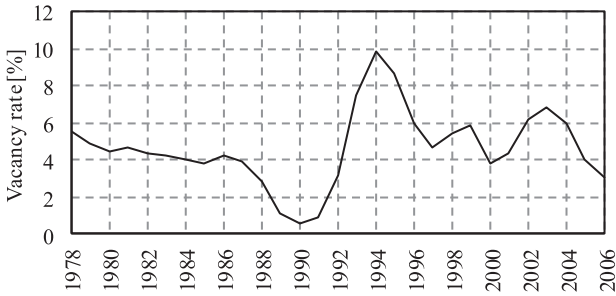


Figure 8. Changes in the vacancy rate of Tokyo office buildings over time.

α of Equation (15) can be calculated according to Equation (16).

$$p_{sek}(j) = (1 - q_{sek})^\alpha \binom{j + \alpha - 1}{j} q_{sek}^j \quad (15)$$

$$q_{sek} = 1 - \frac{\mu_{sek}}{\sigma_{sek}^2}, \quad \alpha = \frac{\mu_{sek}^2}{\sigma_{sek}^2 - \mu_{sek}} \quad (16)$$

Figure 7 shows the calculation results for the office vacancy rate for 20 years using the above model. If the probability of cancellation or the number of months required to search for new tenants increases, the vacancy rate will rise. The vacancy rates at points A, B, and C are 2%, 6%, and 12%, respectively. In order to know the effect of the vacancy rate, we conduct a case study for these three points in the later sections. See Togashi (2018b) for a detailed discussion of the average vacancy rate.

Figure 8 shows changes in the vacancy rate for Tokyo office buildings over the past 40 years (CBRE Japan 2006). The vacancy rate approaches 2% during the bubble market in the 1980s, whereas the rate is around 10% during recessions, as in the first half of the 1990s. In cities other than Tokyo, vacancy rates of around 10% are not uncommon. Therefore, vacancy rates of 2% and 12% (points A and C in Figure 7) can represent vacancy rates during a boom and a recession, respectively.

Finally, by integrating the stochastic models of office worker behavior, tenant characteristics, and tenant replacement, we can simulate the office worker density. Figure 9

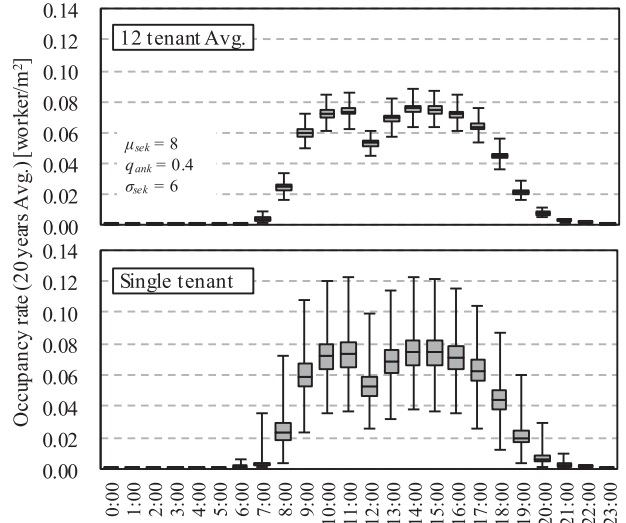


Figure 9. Simulation sample of the occupancy rate change by time of day.

illustrates an example simulation result with a box-plot diagram. In this simulation, the number of tenants is 12, and each tenant rents floor space of 500 m². The upper diagram of the figure shows the result for the average of 12 tenants, and the lower diagram shows that for a single tenant. The swing width is larger in the lower diagram than in the upper diagram because changes of the office worker densities of individual tenants can be offset when the entire building is considered. This distinction matters for our subsequent analyses because HVAC equipment for individual tenants, such as air handling units, is operated under the uncertainty shown in the lower diagram, whereas HVAC equipment installed for the entire building, such as a central heat source machine, is operated under the uncertainty shown in the upper diagram. Therefore, energy conservation investments for these types of equipment do not face equivalent risks, as is discussed in a later section.

2.5. Stochastic model of energy cost

Conversion rates are needed to convert energy consumption to a monetary value. These flat rates may fluctuate over the long term. Figure 10 shows the cost of electricity and gas in Japan over the past 45 years, with the value in 2016 set at 1.0 (METI 2017). The upper panel displays the raw data, and the lower panel shows the moving average over three years decomposed into trend and irregular components. Therefore, the energy costs of electricity and gas (EC_{elc} [yen/kWh] and EC_{gas} [yen/m³], respectively) can each be broken down into a trend component (T_{EC}) and an irregular component (I_{EC}), as shown in Equations (17) and (18). EC_{BSelc} and EC_{BSgas} are the baseline costs of electricity and gas, which are 30 yen/kWh and 100 yen/m³, respectively. As can be seen from the lower panel of Figure 10, the irregular components of electricity

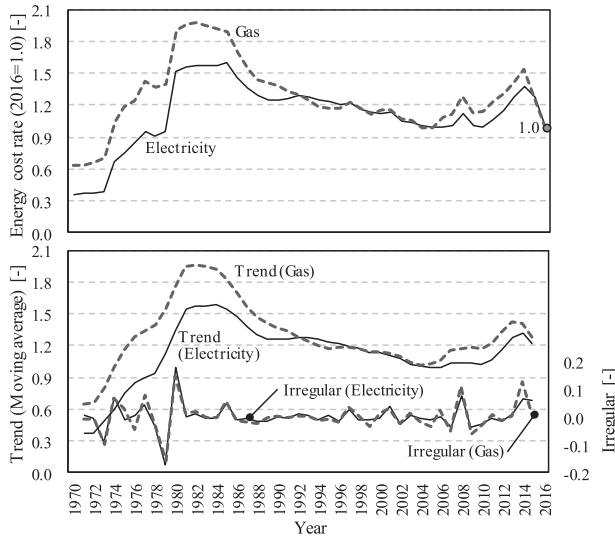


Figure 10. Electricity and gas cost rate in Japan.

and gas do not independently change stochastically but rather have similar tendencies. Therefore, we model these values using a bivariate normal distribution, as shown in Equation (19).

The trend component T_{EC} is set equal to 1.0 in this study. To examine the influence of this factor, it is necessary for the model of buildings and equipment to express trends over time as well. However, our research model does not express the long-term deterioration of performance due to the aging of facilities or improvements in performance due to repairs.

Unlike electricity and gas charges, water charges not tend to fluctuate in the short term in conjunction with international crude oil prices because water charges are mainly affected by changes in the long-term population in the region, the development and aging of water supply facilities, and so on. Because the cost of water differs greatly by region, it is more important to correctly reflect the regional disparity than to correctly reflect the change over time. In this study, the office building considered is assumed to be located in Tokyo, and the costs of water and sewage are each set at 300 yen/m³.

$$EC_{elec}(t) = EC_{BSelec}(T_{EC_{elec}}(t) + I_{EC_{elec}}) \quad (17)$$

$$EC_{gas}(t) = EC_{BSgas}(T_{EC_{gas}}(t) + I_{EC_{gas}}) \quad (18)$$

$$\begin{aligned} \begin{pmatrix} I_{EC_{elec}} \\ I_{EC_{gas}} \end{pmatrix} &= N \left(\begin{pmatrix} \mu_{elec} \\ \mu_{gas} \end{pmatrix}, \begin{pmatrix} \sigma_{elec}^2 & \rho\sigma_{elec}\sigma_{gas} \\ \rho\sigma_{elec}\sigma_{gas} & \sigma_{gas}^2 \end{pmatrix} \right) \\ &= N \left(\begin{pmatrix} 0.00218 \\ 0.00196 \end{pmatrix}, \begin{pmatrix} 0.00233 & 0.00229 \\ 0.00229 & 0.00271 \end{pmatrix} \right) \end{aligned} \quad (19)$$

3. Stochastic energy consumption predictions

In this section, we discuss the implementation of the Monte Carlo method by combining the energy consumption

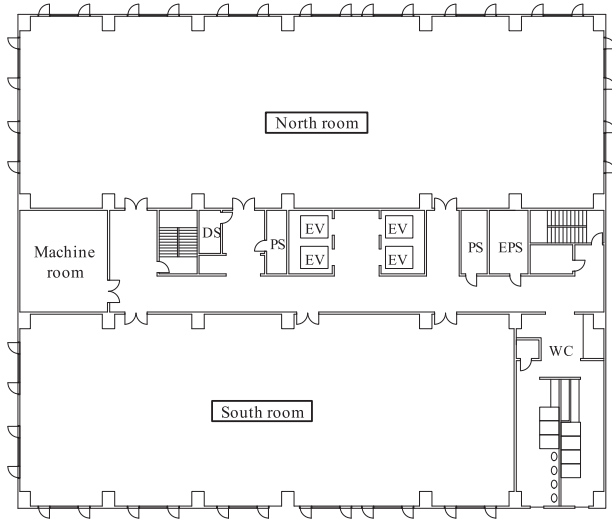


Figure 11. Plan of office.

prediction model with the stochastic models introduced in the previous section. Using this method, we can obtain the energy reduction due to the introduction of energy efficiency equipment as a probability distribution.

3.1. Simulation conditions

The target of the simulation is a seven-story tenant office building located in Tokyo. This is the standard building used in Japan's energy conservation law (i.e. in the Act on Rationalizing Energy Use). Figure 11 shows a reference floor plan. The second to the seventh floors are the tenant floors, and the north and south sides of these floors each have one tenant, so there are twelve tenants in total. As the floor area of each tenant is about 500 m², the total floor space for lending is about 6000 m². Figure 12 shows the heat source and air conditioning systems in this example. The heat source machine includes an air heat source heat pump (AHP) and a direct fired absorption chiller, and it is a two-pump system with a primary and a secondary pump. Two air handling units (AHU: perimeter and interior) are installed for each tenant. Table 4 shows the brief specifications of the HVAC equipment installed into such a building, and further detailed information are provided by the Society of Heating, Air-conditioning and Sanitary Engineers (SHASE) (2016).

Due to space limitations, we do not describe the full building model in detail here but rather discuss only the main calculation methods. We create the simulation model using the program library described by Togashi (2016). The accuracy of the thermal load calculation of this library is verified using BESTEST (Judkoff and Neymark 1995; Togashi and Tanabe 2009), and the accuracy of the HVAC system calculations is verified according to SHASE guidelines (Ono, Ito, and Yoshida 2017; SHASE 2016).

For the heat load calculation, the backward difference is used with a time step of one hour. The zone is divided

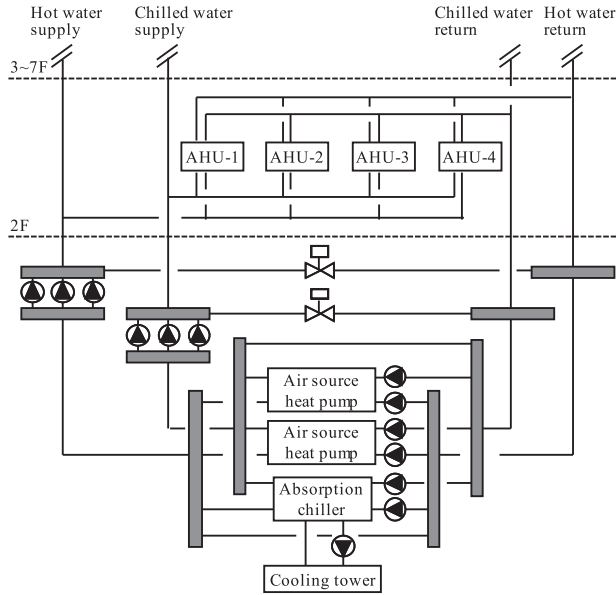


Figure 12. Heat source and air conditioning system.

into interior and perimeter zones, and we calculate the radiant heat transfer and ventilation between the zones. Mass points are set for each zone and each layer of the wall. The solar radiation through a window is calculated based on the incident angle characteristics of the glass. We also calculate the solar radiation shielding effect due to the opening and closing of blinds.

The heat source and air conditioning system is expressed by combining sub-models, which include an air heat source heat pump, a direct fired absorption chiller, a cooling tower, a pump, and an air handling unit. The variables passed between these sub-models are solved using the quasi-Newton method. The input ratio of the heat pump, the flow and pressure characteristics of the pump and the fan, the regenerator, and the resistance of ducts or pipes are expressed by their characteristic formulas. The direct fired absorption chiller, cooling tower, and cold / hot water coil are all expressed by physical

formulas. The amount of power generated by solar cells is calculated according to Japanese Industrial Standards C8907.

We also calculate the water consumption of a toilet bowl to evaluate the amount of water conserved by using water-saving toilets. The daily water usage of a toilet bowl, W_{dy} , can be expressed using Equation (20). R is the number of times the toilet is used, W is the water consumption per use, the subscript *cls* indicates a flush toilet, and the subscript *unl* indicates a urinal. Different parameters are used for men and women.

$$W_{dy} = H_{sty}(R_{unl}W_{unl} + R_{cls}W_{cls}) \quad (20)$$

Figure 13 shows the results of the annual primary energy consumption simulation. The results for several programs described in the above guidelines are also shown. The annual primary energy consumption is 223 MJ/(m²yr), which is typical for office buildings in Tokyo, and the energy consumption levels for the evaluated programs are comparable to other results. For this verification, we use the boundary conditions described in the guidelines, but for our analysis using the Monte Carlo method, we replace these boundary conditions with the output of the stochastic model introduced in section 2.

In all, we consider five energy conservation investments: a high-efficiency heat source, CO₂-based ventilation control, a total heat exchanger, water-saving toilets, and a photovoltaics panel, which we denote as A, B, C, D, and E hereafter. Table 5 shows the costs and calculation methods for these investments.

3.2. Probability distribution of energy consumption

We next calculate the probability distributions of energy reductions using the Monte Carlo method. As mentioned, the boundary conditions are generated using the stochastic model developed in the previous section. We set the parameters based on the assumption of an average vacancy

Table 4. Specifications of main equipment.

Equipment	Specification	Number
Absorption chiller	Cooling capacity: 527 kW, Heating capacity: 346 kW, Gas consumption: 32.4 m ³ /h	1
Cooling tower	Cooling capacity : 939.4 kW, Fan electricity: 7.5 kW	1
Chilling water and hot water primary pump	Flow rate: 1512 L/min, Pressure rise: 147 kPa, Electricity: 7.5 kW	2
Cooling water pump	Flow rate: 2693 L/min, Pressure rise: 245 kPa, Electricity: 18.5 kW	1
Air heat source heat pump	Cooling capacity: 300 kW, Heating capacity: 300 kW, Electricity: 99.6 kW	2
Chilling water and hot water primary pump	Flow rate: 860 L/min, Pressure rise: 147 kPa, Electricity: 3.7 kW	4
Chilling water and hot water secondary pump	Flow rate: 1077 L/min, Pressure rise: 245 kPa, Electricity: 11.0 kW	6

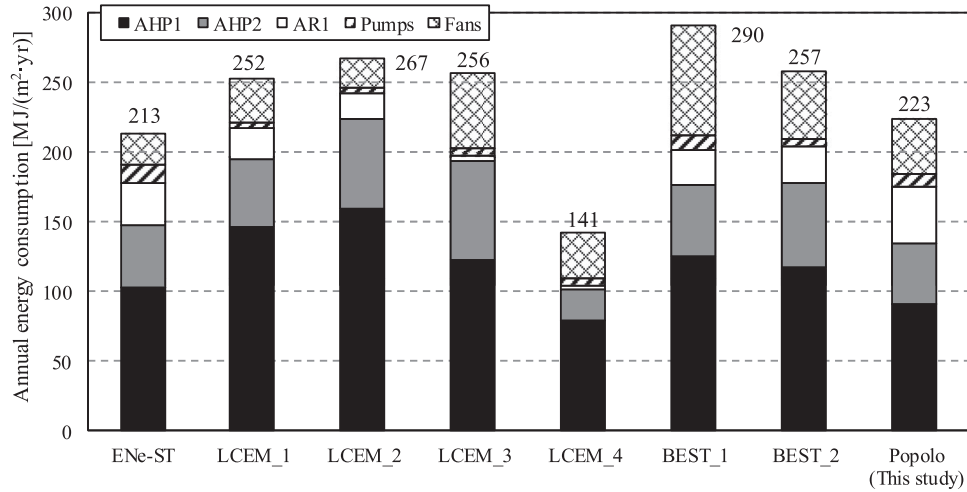


Figure 13. Calculation results of annual primary energy consumption.

Table 5. Costs and calculation methods for energy conservation investments.

Method	Cost [yen]	Calculation method
A: High-efficiency heat source	2,600,000	Air heat source heat pump:Chilling COP and heating COP are changed from 3.0 to 4.5 and 3.0 to 3.5, respectively. Absorption chiller:Improving efficiency at partial load by installing inverter control of refrigerant
B: CO ₂ -based ventilation	7,200,000	Controlling ventilation volume with number of occupants. CO ₂ generated by humans is fixed at 0.02 m ³ /(person/h). Fresh air CO ₂ level is fixed at 400 ppm.
C: Total heat exchanger	12,000,000	Heat exchange efficiency is 70%. Supply air fan and return air fan pressures are changed from 850 to 1050 Pa and 350 to 550 Pa, respectively.
D: Water-saving toilets	3,000,000	Water use of closet and urinal are changed from 8.0 to 3.8 L/flush and 2.8 to 0.8 L/flush, respectively.
E: Photovoltaics panels	16,200,000	Surface area: 300 m ² , power generation efficiency: 18%, Angle: 30°

rate of 6% (Point B in Figure 7). The period of heating runs from November to April, and the period of cooling runs from May to October. When overtime workers are present, the lights remain on. However, air conditioning stops running at the end of business hours. Through repeated calculations, we generate 1000 predicted energy consumption values.

Figure 14 shows the distribution of annual primary energy consumption based on the results of 1000 simulations. The distribution spread occurs because energy consumption is affected by the weather and the tenants' conditions. The difference between the maximum and minimum energy consumption is doubled, and the impacts of energy efficiency investments are affected by this uncertainty. Figure 15 illustrates the distribution of the partial load operations of AHP and AHU (No. 4-1) using a box-plot diagram. The left panel shows the cooling operation, and the right panel shows the heating operation. Compared with AHP, the variation in the occurrence of AHU

becomes very large when the partial load is less than 40% for both cooling and heating operations for the same reason as that explained earlier regarding the variation in the occupancy rate (Figure 9). The AHP load is determined by a combination of activities of various tenants, whereas the AHU load is greatly affected by the characteristics of a single tenant. Therefore, introducing inverters for AHU for individual tenants and introducing inverters in heat source equipment are both energy efficiency investments for low-load operations, but they are strictly unequal in value. The introduction of inverters to individual AHUs has more risk. Figure 16 illustrates the distribution of daily water usage per floor. For the same reason explained above, the variation in water consumption for a specific floor is very large compared with that of the whole building. Therefore, the value of introducing water-saving equipment for individual tenants differs from that of introducing a wastewater recycling system or high efficiency pumps for the whole building.

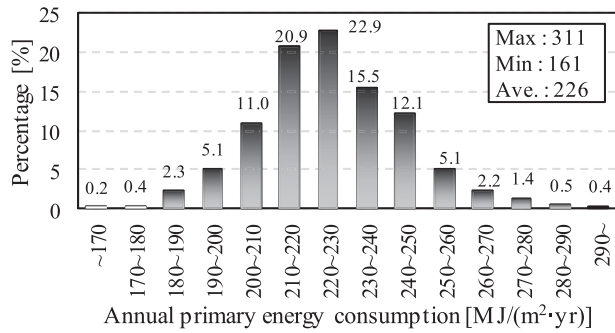


Figure 14. Distribution of annual primary energy consumption.

In order to quantitatively evaluate the risk arising from these uncertainties, we apply financial engineering methods to these calculation results, as discussed in the next section.

4. Evaluation with financial engineering methods

4.1. Method of monetary conversion

The cost reduction in month m in the i th calculation is expressed by Equation (21), where CF , FR , and RD are the cash flow, flat rate, and energy reduction, respectively. The maintenance cost strictly depends on the type and scale of equipment, but, on average, it is said to be about 1.5% of the initial investment amount (Technical Committee on Electric Air Conditioning 1992). Therefore, in this study, we also assume that 1.5% of the initial investment amount is expensed every year. The present value of these cash flows over 20 years (240 months), the DCF, is given by Equation (22). Since there is a risk that the cash flow drops too low, a risk premium (rp) is added to the interest rate Y . In an established market, like those for shares and bonds, the risk premium can be assessed using the capital asset pricing model (CAPM). However, there are not enough cases of energy efficiency investments to use this approach,

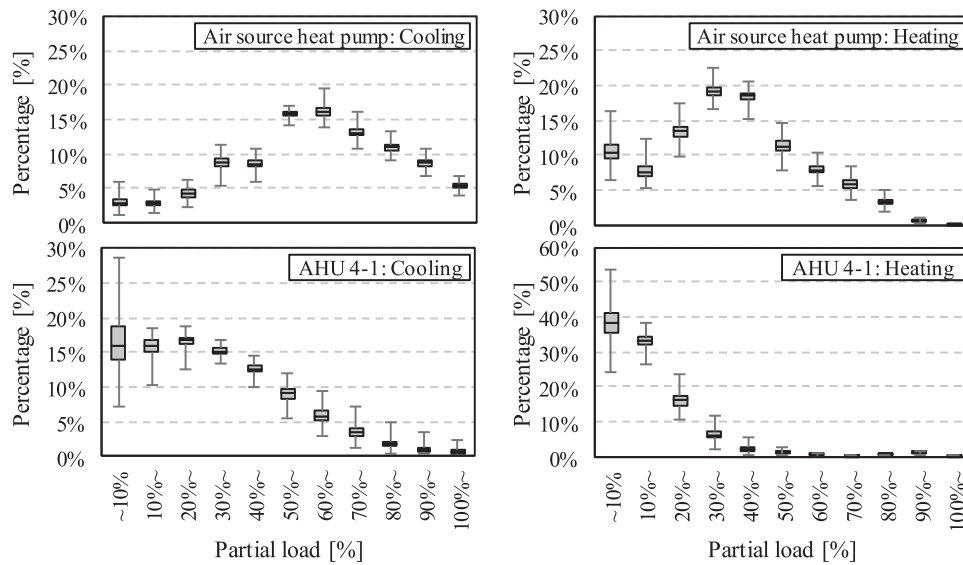


Figure 15. Distribution of partial load operations.

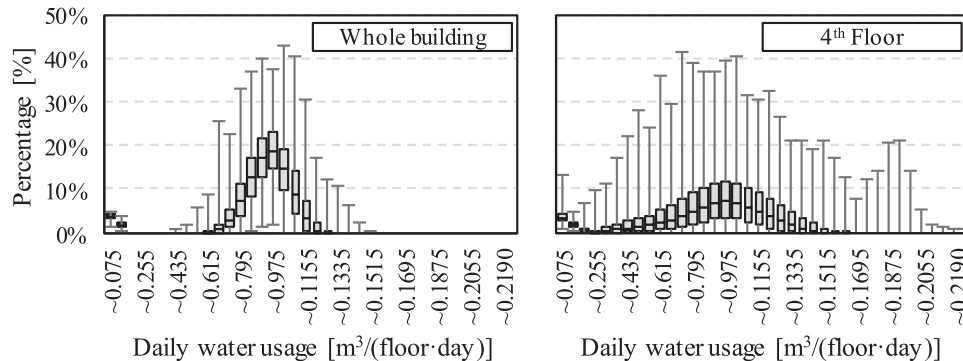


Figure 16. Distribution of daily water usage per floor.

Table 6. Correlation coefficient of the reduction in utility cost by each energy efficiency investment.

	O ₁	O ₂	O ₃	O ₄	A	B	C	D	E
O ₁ : Total number of months tenants stayed	1.000	0.196*	-0.015	0.034	0.219*	0.071*	0.081*	0.176*	0.031
O ₂ : Total number of occupants	-	1.000	0.042	-0.016	0.231*	-0.322*	-0.335*	0.956*	-0.016
O ₃ : Average outdoor temperature	-	-	1.000	0.014	0.178*	0.042	-0.050	0.030	-0.006
O ₄ : Total global horizontal radiation	-	-	-	1.000	-0.016	-0.031	-0.046	-0.021	0.995*
A: High-efficiency heat source	-	-	-	-	1.000	-0.137*	-0.280*	0.228*	-0.029
B: CO ₂ -based ventilation	-	-	-	-	-	1.000	0.977*	-0.308*	-0.038
C: Total heat exchanger	-	-	-	-	-	-	1.000	-0.322*	-0.049
D: Water-saving toilets	-	-	-	-	-	-	-	1.000	-0.019
E: Photovoltaics panels	-	-	-	-	-	-	-	-	1.000

* $p < 0.05$.

and it is difficult to assess a risk premium from market information.

$$CF_{i,m} = RD_{elc,i,m}FR_{elc} + RD_{gas,i,m}FR_{gas} + RD_{wat,i,m}FR_{wat} + RD_{swg,i,m}FR_{swg} \quad (21)$$

$$DCF_i = \sum_{m=0}^{240} CF_{i,m} \frac{1}{(1 + Y + rp)^{m/12}} \quad (22)$$

4.2. Evaluation of stochastic characteristics

We simulate the probability distributions of energy costs that are reduced by the five energy efficiency investments mentioned in the previous section. Table 6 shows the correlation coefficient of the reduction in utility cost due to each energy efficiency investment. The correlation coefficients for tenant conditions (O₁ and O₂) and weather conditions (O₃ and O₄) are also shown in Table 6.

O₁ has the greatest impact on real estate value. Investments A and D have positive correlations with O₁, whereas investments B, C, and E have little correlation with O₁. In the case of multiple investment assets, risk can be reduced by combining investments that are not positively correlated, as we discuss later. Therefore, investments C, D, and E are more advantageous than A and B are for reducing the risk of the real estate business.

The existence of a tenant implies that of office workers, but the correlation coefficient between O₁ and O₂ is 0.196, which is not high. This result is reasonable, however, because the number of office workers differs for each tenant in this model. O₂ is highly correlated with D, which suggests that, although the number of toilet flushes is influenced by the number of office workers and their work hours, the influence of the former is larger. A is also positively correlated with O₂, but the correlation is small because, unlike a toilet, a heat source system cannot completely shut off even when few people are present. B has a negative correlation with O₂ because, when the office worker density is high, the amount of ventilation cannot be reduced by the level of CO₂. C also has a negative correlation with O₂ because a large number of office workers

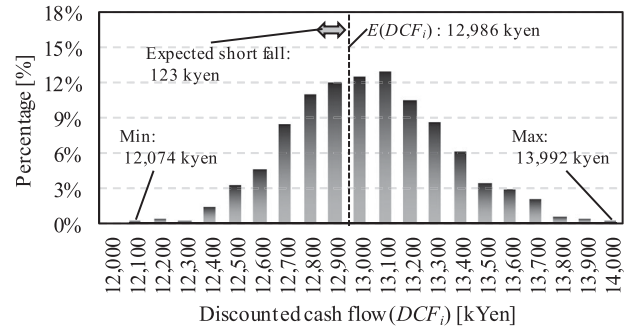


Figure 17. Distribution of the discounted cash flow.

generates a large amount of internal heat, so it is better to introduce outside air directly during the cool season. Thus, a total heat exchanger is only effective over a shorter time period.

4.3. Estimation of the risk premium for each energy efficiency investment

Figure 17 shows the calculation results for the DCF_i distribution setting rp equal to zero in Equation (22) in the case of investment A. The distribution spreads to the left and right, and there is a risk that the realized value is lower than the average value $E(DCF_i)$. The expected value of this downside of the distribution is expressed by Equation (23) and is called the expected shortfall (ES). Dividing the ES by $E(DCF_i)$ gives the risk associated with the present value of one unit of investment, which is the risk premium rp (Equation (24)). The interest rate Y in Equation (22) can be calculated using the weighted average cost of capital (WACC). In 2017, the average interest-bearing debt of a Japan real estate investment trust (J-REIT) was lower than 0.8% (Kawai 2017), and the average dividend yield on a J-REIT for a Tokyo office building was about 3.5%. The office building considered in this study is smaller than the average investment property owned by a J-REIT, and the risk cannot be diversified by a portfolio, so the applicable rates are slightly higher than these example rates for J-REITs. Therefore, in this study, the ratios and interest

Table 7. Risk premia for energy efficiency investments (Base case).

	A: High-efficiency heat source	B: CO ₂ -based ventilation	C: Total heat exchanger	D: Water-saving toilets	E: Photo-voltaics panels
Average value $E(DCF_i)$	13,557 kYen	22,093 kYen	11,615 kYen	22,597 kYen	29,274 kYen
Maximum value	12,699 kYen	16,765 kYen	8130 kYen	18,375 kYen	27,826 kYen
Minimum value	14,435 kYen	26,360 kYen	14,348 kYen	26,960 kYen	30,671 kYen
Expected shortfall ES	105 kYen	506 kYen	345 kYen	519 kYen	188 kYen
Risk premium rp	0.78%	2.29%	2.98%	2.30%	0.64%
Discount rate ($i + rp$)	3.58%	5.09%	5.78%	5.10%	3.44%

Table 8. Risk premia when the vacancy rate and probability model are changed.

Case	Weather data	Tenant and occupant	Energy cost	Vacancy rate	Energy efficiency investments				
					A	B	C	D	E
1	random	random	random	6%	0.94%	2.51%	3.79%	2.37%	0.90%
2	random	random	random	2%	0.89%	2.55%	3.81%	2.37%	same as case 1
3	random	random	random	12%	0.96%	2.35%	3.55%	2.58%	same as case 1
4	constant	random	random	6%	0.69%	2.22%	4.15%	same as case 1	0.50%
5	random	constant	random	6%	0.65%	1.06%	1.27%	no risk	same as case 1
6	random	random	constant	6%	0.82%	2.48%	3.76%	2.37%	0.74%

rates for debt and equity are assumed to be 40% and 60% and 1.0% and 4.0%, respectively. The WACC is therefore calculated as 2.8% ($40\% \times 1.0\% + 60\% \times 4.0\%$).

$$ES = E(DCF_i | DCF_i < E(DCF_i)) \quad (23)$$

$$rp = \frac{ES}{E(DCF_i)} \quad (24)$$

Table 7 shows the results of calculating the risk premium for each energy efficiency investment. As mentioned above, the tenant vacancy rate is assumed to be 6% (point B in Table 7). Investment E has the lowest risk because the amount of solar radiation is stable from year to year even though the weather on any given day may be cloudy or sunny. Investment A is lower risk than investments B and C are. This result can be explained in Figure 9 in the previous section. Since B and C are installed into individual air handling units, they are greatly affected by each tenant. In contrast, A is provided for the entire building, so the uncertainties of individual tenants are canceled out and stabilized. Finally, investment D has a high-risk premium because it is strongly affected by the number of office workers, as shown in Table 6.

To clarify the influence of the fluctuation of each stochastic model on the value of the investments, the risk premia were recalculated by replacing the stochastic model with fixed boundary conditions and changing the vacancy rate. The results of this recalculation are shown in Table 8. The risk premia for investments A, B, C, and D differ by about 0 to 0.3 points depending on the vacancy rates (case 2 and 3), and these effects are smaller than the influence of the existence of three stochastic models on the risk

premia (case 4, 5, 6). Weather uncertainty affects the risk premium of each energy efficiency investment, but it has a particularly large impact on photovoltaics panels. Tenant occupancy uncertainty greatly influences the risk premia of energy efficiency investments in AHUs (B and C) but has a smaller influence on the risk premium of an investment in the heat source (A). The explanation provided for Figure 9, Figures 15 and 16 applies here as well; the uncertainties of individual tenants are offset in the case of heat sources but not in the case of individual AHUs.

4.4. Optimal investment ratio for energy efficiency investments

As mentioned earlier, Monte Carlo simulation enables us to evaluate both the risk of and return to each energy efficiency investment. Problems related to existing energy efficiency investment may also be solved with this information using financial engineering methods. For example, it is said that the energy service company (ESCO) business has a problem of cream skimming. ESCO businesses are generally financed using one of two methods: “shared savings” and “guaranteed energy savings.” The former is funded by the owner, and the latter is funded by the ESCO. Therefore, general investors do not directly appear in the ESCO business. Due to this lack of access to financial resources, especially in shared saving contracts, ESCOs prefer very short payback periods, leading to lost opportunities for investment, which create the cream skimming problem mentioned above (Langlois and Hansen 2012). One effective solution to this problem is to allow general investors to participate in addition to owners and ESCOs.

Table 9. Initial costs of energy efficiency investments.

Energy efficiency investment	Initial cost	Basis
A: High-efficiency heat source	2,600,000	Difference from highly efficient models
B: CO ₂ -based ventilation	7,200,000	300 thousand yen per one air handling unit
C: Total heat exchanger	10,500,000	AHU unit price: 295 - > 365 yen / CMH
D: Water-saving toilets	3,000,000	Difference between water-saving type and general type
E: Photovoltaics panels	16,200,000	300,000 yen / kW

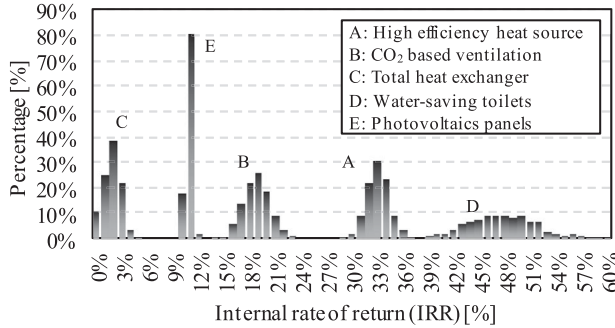


Figure 18. Distribution of the IRR.

To do so, several ESCO projects need to be bundled and securitized. In the future, when such securitization is realized, it is necessary to optimally combine the many ESCO projects (energy efficiency investments).

If the covariances of the IRRs of each energy efficiency investment are calculated, we can obtain an optimal investment ratio using modern portfolio theory (Markowitz 1952). Thus, we solve Equation (25) for IRR , where I is the initial investment. Table 9 shows the costs of the investments. The covariances of the IRRs of each energy efficiency investment are calculated based on these initial costs and 1000 simulation results.

$$I = \sum_{m=0}^{240} CF_{i,m} \frac{1}{(1 + IRR)^{m/12}} \quad (25)$$

Figure 18 shows the distribution of the IRR for each energy efficiency investment, and Table 10 shows the averages and standard deviations of the investments. The IRR of investment D is high, but it also has a large variation. By contrast, investment E has low average values and a small variation. A traditional building energy simulation

that only evaluates the average IRRs would conclude that it is optimal to invest in D, B, A, E, and C, in that order, until funds run out. However, in this study, we show how to reduce risk by combining each investment.

The expected rate of return and standard deviation of a portfolio combining n investments can be expressed by Equations (26) and (27), where r_n , w_n , σ_n^2 , and σ_{nm} are the expected rate of return, the combining ratio, the variance of the n^{th} investment, and the covariance of the n^{th} and m^{th} investment, respectively.

$$r_{PF} = \sum_{i=0} w_i r_i \quad (26)$$

$$\sigma_{PF} = \sum_{i=0} \sum_{j=0} w_i w_j \sigma_{ij} \quad (27)$$

Here, we assume that investors are risk averse. This assumption means that investors prefer a high expected rate of return per standard deviation, which means they prefer a portfolio in the upper left of Figure 19. The combining ratio at which the variance of the portfolio is the smallest with respect to a given expected rate of return can be calculated with Equation (28).

$$\begin{bmatrix} \sigma_{11} & \sigma_{12} & \cdots & \sigma_{1n} & -r_1 & -1 \\ \sigma_{21} & \sigma_{22} & \cdots & \sigma_{2n} & -r_2 & -1 \\ \vdots & \vdots & \ddots & \vdots & \vdots & \vdots \\ \sigma_{n1} & \sigma_{n2} & \cdots & \sigma_{nn} & -r_n & -1 \\ r_1 & r_2 & \cdots & r_n & 0 & 0 \\ 1 & 1 & \cdots & 1 & 0 & 0 \end{bmatrix} \begin{bmatrix} w_1 \\ w_2 \\ \vdots \\ w_n \\ \lambda \\ \theta \end{bmatrix} = \begin{bmatrix} 0 \\ 0 \\ \vdots \\ 0 \\ r_{PF} \\ 1 \end{bmatrix} \quad (28)$$

Using Equations (26) to (28) and defining r_n and σ_n as the average and standard deviation of the IRR, the expected rate of return and standard deviation of a combination of

Table 10. Average and standard deviation of the IRR.

	Standard deviation			Average		
	Vacancy rate = 2%	6%	12%	Vacancy rate = 2%	6%	12%
A: High-efficiency heat source	1.22%	1.28%	1.40%	33.2%	32.6%	31.8%
B: CO ₂ -based ventilation	1.63%	1.57%	1.55%	18.6%	18.3%	18.0%
C: Total heat exchanger	1.04%	1.02%	1.17%	1.5%	1.3%	1.0%
D: Water-saving toilets	4.23%	4.22%	4.40%	49.2%	47.4%	44.8%
E: Photovoltaics panels	0.33%	10.3%				

Table 11. Variance-covariance matrix of energy efficiency investments (Vacancy rate = 6%).

	A: High-efficiency heat source	B: CO ₂ -based ventilation	C: Total heat exchanger	D: Water-saving toilets	E: Photovoltaics panels
A: High-efficiency heat source	0.01645	0.00365	-0.00077	0.00753	0.00106
B: CO ₂ -based ventilation	-	0.02451	0.01228	-0.01472	0.00047
C: Total heat exchanger	-	-	0.01031	-0.00551	0.00012
D: Water-saving toilets	-	-	-	0.17798	0.00056
E: Photovoltaics panels	-	-	-	-	0.00108

multiple energy efficiency investments can be calculated. Unlike stocks, energy efficiency investments in building facilities cannot be sold short, so w_n is set to be greater than zero.

Table 11 shows the variance-covariance matrix of the energy efficiency investments, and Figure 19 shows the averages and standard deviations of the IRRs of single investments and portfolios. The thin curve in Figure 19 reflects a combination of two investments. When the covariance between the two investments is negative, as in the case of investments B and D, the expected rate of return per standard deviation can be greatly improved by combining the two investments, as shown in the figure. In contrast, when two investments are positively correlated, as in the case of investments B and C, the expected rate of return per standard deviation hardly changes even when the two investments are combined. The optimal investment allocation calculated using Equation (28) is the thick curve on the upper left side of Figure 19. This curve is generally called the efficient frontier.

In the case of raising funds at the interest rate Y , the negative cash flow of interest rate Y can be avoided with certainty by choosing not to invest. The position obtained by this selection is the point in Figure 19 at which the standard deviation is zero and the expected rate of return is Y . Y_1 is the point at which the interest is 2.8%, and Y_2 is that at which the interest rate is 8.0%. The optimal investment must be chosen over all positions, including those that do not invest. Therefore, the allocation that maximizes the expected rate of return per standard deviation is a tangent drawn from Y_1 or Y_2 to the efficient frontier. These contact points T_1 or T_2 are called tangency portfolios.

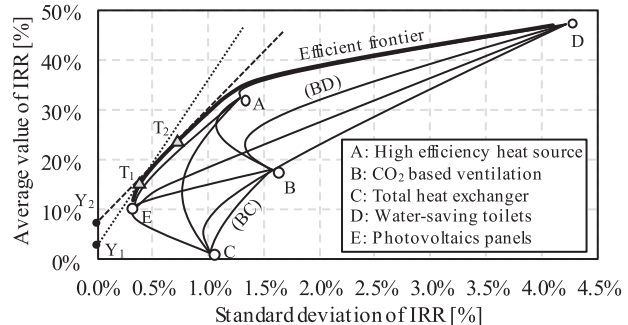


Figure 19. Average and standard deviation of IRR of each energy efficiency investment and portfolio.

The allocation ratio of energy efficiency investments at points T_1 and T_2 , the standard deviation, and the expected rate of return of the portfolio are shown in Table 12. The effect of the vacancy rate is much smaller than that of the interest rate. The expected rate of return per standard deviation is larger in this case than when concentrating on a single investment. When the interest rate is low (Y_1), it is effective to increase the proportion of investment in E, which has a low variation and high accuracy. In contrast, when the interest rate is high (Y_2), it is effective to increase the proportion of investment in high-risk, high-return energy efficiency projects.

The average IRR value of investment E is 10.3%, so, when the interest rate is 8.0% (Y_1), this investment provides a profit of only 2.3%. However, the optimal investment allocation ratio in investment E is about 40%, which is not small. We obtain this result because the probabilistic characteristics of the IRR of investment E are different

Table 12. Optimum investment allocation ratio calculated by portfolio theory.

	Y_1 (interest rate = 2.8%)			Y_2 (interest rate = 8.0%)		
	Vacancy rate = 2%	6%	12%	Vacancy rate = 2%	6%	12%
A: High-efficiency heat source	20.54%	18.02%	15.17%	47.41%	42.22%	36.70%
B: CO ₂ -based ventilation	7.35%	6.64%	7.40%	12.60%	11.47%	12.98%
C: Total heat exchanger	0.00%	0.00%	0.00%	0.00%	0.00%	0.00%
D: Water-saving toilets	3.59%	3.12%	2.52%	7.25%	6.42%	5.25%
E: Photovoltaics panels	68.52%	72.22%	74.91%	32.75%	39.88%	45.07%
Portfolio expected rate of return	17.00%	16.00%	15.00%	25.00%	23.00%	21.00%
Portfolio standard deviation	0.42%	0.40%	0.39%	0.72%	0.68%	0.66%

from those of the other energy efficiency investments, so combining other investments with investment E reduces the overall risk. For the same reason, the allocation ratio in investment B is not 0% even though its expected rate of return per standard deviation is smaller than those of the other investments. On the other hand, the investment allocation ratio for investment C is 0% because the probability characteristics of investment C are similar to those of investment B, so investment B, which has a higher expected rate of return than investment C has, is given priority.

5. Conclusions

The impact of an energy efficiency investment is affected by the operating conditions of the equipment related to that investment. As shown in Figures 15 and 16, the uncertainty of the operating conditions of the equipment is affected by the building zone targeted by the equipment. If the equipment handles many zones, the characteristics of each zone are canceled and stabilized, but if the equipment covers only a few zones, the operating conditions are greatly affected by the special natures of these few zones. Therefore, risk assessment becomes relatively important when the investment target is equipment covering a small number of zones. It should be noted, however, that operating conditions cannot be offset even when the equipment covers many zones if all zones behave similarly. Because this analysis considered a tenant office building, the differences in behaviors across tenants were effective in stabilizing the load on the entire building, but in the case of a self-owned building, this effect is expected to be small. On the contrary, a commercial tenant building has greater loads differences across tenants than a tenant office building does, so the risk reduction effect on the entire building is large.

As shown in Table 7, if the uncertainty of the energy-saving effect of individual equipment is reflected in the calculation, the risk premium is different for each investment. For example, in Table 7, the discount rates of the high-efficiency heat source and the total heat exchanger are 3.58% and 5.78%, respectively. Capitalizing the cash flow using these values produces a difference of over 60% in the current value. This difference is not reflected at all by the traditional payback period method, and there is a possibility that relatively high-risk investments may be carried out in reality. The effect of uncertainty on the risk premium depends on the characteristics of the equipment associated with the investment. For example, according to the results of this study, photovoltaics panels are most affected by outside air conditions, but total heat exchangers and CO₂-based ventilation are most affected by the uncertainty of tenants' behavior. Since it is not realistic to perform calculations using all possible probabilistic models for each type of energy efficiency equipment, it is necessary to clarify the stochastic events to which each facility is susceptible.

For example, this study indicates that unless tenant behavior is treated stochastically, the discount rates of total heat exchangers and CO₂-based ventilation deviate by 2 to 3%. On the other hand, the discount rate shifts by only 0.3 to 0.5% if weather conditions are not treated stochastically.

The 2% and 12% vacancy rates used in the vacancy rate sensitivity analysis express two extreme market conditions in Japan, as explained in Figure 8. As shown in Table 8, however, the influence of these values on the discount rate is less than 1%, which is not very large. In Case 4 in the same table, the discount rate changes greatly, meaning that the influence of occupant behavior is large. In particular, Japan has large numbers of overtime and holiday workers, and the facility operations for these workers are likely to have a large influence on the results of this analysis. For example, in this study, lights are kept on during overtime periods, but the air conditioning stops running; uncertainty will increase if air conditioning is also operated for overtime workers.

The probabilistic characteristics of energy conservation investments obtained by the methods used in this study allow for different investigations from those using conventional methods by using financial engineering methods. The problem of optimal investment allocations considered in this analysis is a typical example. By applying this method rather than the simple payback period method, we find different optimal investment orders depending on the magnitude of the interest rate and the correlations between energy efficiency investments, as shown in Table 12. However, in reality, investment in one building is too small scale, and the investment amount cannot be adjusted continuously. In addition, constructing this research model research is very time consuming, and the calculation load is very large. For example, in this study, we obtain a stochastic distribution by performing a 20-year simulation for 10,000 m² office buildings 1000 times, and this simulation took about ten hours for each case. The central processing units used to perform simulation was an Intel Core i7-5820, which is a high-end processor capable of parallel calculation of 12 threads. Increasing the number of energy efficiency investments investigated increases the calculation time. For some time, such studies have only been possible at the research level and are impossible in the context of daily design work. However, now that computers are evolving to strengthen parallelization, the computing environment for repeating an independent calculation many times using the Monte Carlo method, as in this analysis, will continue to improve. Real-option evaluation can be expected as an application of the stochastic characteristics obtained by this analysis. For example, although the simulation period was set to 20 years in this study, in reality, a typical HVAC system is used for more than 20 years. Thus, a real-option valuation could be performed to evaluate the replacement of HVAC equipment.

In this study, the risk levels of energy efficiency investments in a building are evaluated using the Monte Carlo method. In order to apply the Monte Carlo method, the boundary conditions of the building energy simulation, which are the weather process, office worker behavior, tenants' characteristics, and tenant replacement, are represented by stochastic models. Using these stochastic models, we run repeated energy simulations to predict the probability distributions of energy reduction amounts. Based on the expected shortfall, we calculate the risk premia needed to discount the utility costs reduced by each energy-saving investment along with the variance and covariance matrix of the IRRs of each energy efficiency investment. Based on this matrix, we apply modern portfolio theory to determine the optimal energy efficiency investment allocation ratio considering the risk associated with each investment.

Acknowledgements:

This work was supported by JSPS KAKENHI Grant Numbers JP 16K18198 and JP 18K04462.

Funding

This work was supported by JSPS KAKENHI [grant number JP 16K18198], [grant number JP 18K04462].

References

- Abadie, L. M., J. M. Chamorro, and M. González-Eguino. 2013. "Valuing Uncertain Cash Flows from Investments That Enhance Energy Efficiency." *Journal of Environmental Management* 116: 113–124. doi:10.1016/j.jenvman.2012.09.030.
- Agency for Natural Resources and Energy, Ministry of Economy, Trade, and Industry (METI) Japan. 2017. Japan's Energy White Paper 2017.
- Ansar, J., and R. Sparks. 2009. "The Experience Curve, Option Value and the Energy Paradox." *Energy Policy* 37 (3): 1012–1020. doi:10.1016/j.enpol.2008.10.037.
- Appraisal Institute. 2013. *The Appraisal of Real Estate 14th Edition*. ISBN978-1-935328-38-4
- Cano, E. L., M. Groissöck, J. M. Moguerza, and M. Stadler. 2014. "A Strategic Optimization Model for Energy Systems Planning." *Energy and Buildings* 81: 416–423. doi:10.1016/j.enbuild.2014.06.030.
- Cano, E. L., J. M. Moguerza, and A. Alonso-Ayuso. 2016. "A Multi-Stage Stochastic Optimization Model for Energy Systems Planning and Risk Management." *Energy and Buildings* 110: 49–56. doi:10.1016/j.enbuild.2015.10.020.
- CBRE Japan. 2006. "Bubble Period and Current Rent Volatility." Accessed March 20, 2018. https://www.cbre-propertysearch.jp/article/the_next_bubble-2006-vol3.
- Chegut, A., P. Eichholtz, and N. Kok. 2014. "Supply, Demand, and the Value of Green Buildings." *Urban Studies* 51 (1): 22–43. doi:10.1177/0042098013484526.
- DeCanio, S. J. 1993. "Barriers with in Firms to Energy-Efficient Investments." *Energy Policy* 21 (9): 906–914.
- Eichholtz, P., N. Kok, and J. M. Quigley. 2010. "Doing Well by Doing Good? Green Office Buildings." *American Economic Review* 100 (5): 2492–2509.
- Eichholtz, P., N. Kok, and J. M. Quigley. 2013. "The Economics of Green Building." *Review of Economics and Statistics* 95 (1): 50–63. doi:10.1162/REST_a_00291.
- Fuerst, F., and P. McAllister. 2011a. "Green Noise or Green Value? Measuring the Effects of Environmental Certification on Office Values." *Real Estate Economics* 39 (1): 45–69. doi:10.1111/j.1540-6229.2010.00286.x.
- Fuerst, F., and P. McAllister. 2011b. "Eco-labeling in Commercial Office Markets: Do LEED and Energy Star Offices Obtain Multiple Premiums?" *Ecological Economics* 70 (6): 1220–1230. doi:10.1016/j.ecolecon.2011.01.026.
- Fujii, S., S. Yoshizawa, M. Narasaki, T. Irie, Y. Ota, O. Nanno, M. Moriyama, Y. Okura, and N. Shimizu. 1980. "Kanki setubi sekkei ni okeru hituyou kankiryou santei no tame no zaishitusha mitudo oyobi sono hendou no hyoujunchi sakusei kenkyu (in Japanese) [Investigation of Standard Value of Density and Variation of Occupants for Design of Ventilation Volume]." *Technical Papers of the Annual Meeting of the Society of Heating, Air-conditioning and Sanitary Engineers of Japan*, C-26: 437–440. doi:10.18948/shasetaikai.1981.0_437.
- Gaetani, I., J. Hoes, and J. Hensen. 2016. "Occupant Behavior in Building Energy Simulation: Towards a Fit-for-Purpose Modeling Strategy." *Energy and Buildings* 121 (1): 188–204. doi:10.1016/j.enbuild.2016.03.038.
- Gillingham, K., and K. Palmer. 2014. "Bridging the Energy Efficiency Gap: Policy Insights From Economic Theory and Empirical Evidence." *Review of Environmental Economics and Policy* 8 (1): 18–38. doi:10.1093/reep/ret021.
- International Energy Agency. 2008. *Worldwide Trends in Energy use and Efficiency*. New Milford, Connecticut, USA: Turpin Distribution.
- Jackson, J. 2008. *Energy Budgets at Risk (EBaR): A Risk Management Approach to Energy Purchase and Efficiency Choices*. Wiley. ISBN978-0470197677.
- Jackson, J. 2010. "Promoting Energy Efficiency Investments with Risk Management Decision Tools." *Energy Policy* 38: 3865–3873. doi:10.1016/j.enpol.2010.03.006.
- Judkoff, R., and J. Neymark. 1995. "International Energy Agency Building Energy Simulation Test (BESTEST) and Diagnostic Method." *NREL/TP-472-6231*.
- Kariya, T., Y. Kato, T. Uchiyama, and T. Suwabe. 2005. "Tenant Management and Lease Valuation for Retail Properties: A Real Options Approach." *International Real Estate Review* 8: 44–82.
- Kawai, N. 2017. "J-REIT Market in the First Half of 2017 and Prospective View." *The Journal of Capital Markets Research Institute* 384 (8): 36–43.
- Langlois, P., and S. J. Hansen. 2012. *World ESCO Outlook*. Fairmont Press. ISBN978-1466558144.
- Markowitz, H. 1952. "Portfolio Selection." *The Journal of Finance* 7 (1): 77–91. doi:10.1111/j.1540-6261.1952.tb01525.x.
- Miller, N., J. Spivey, and A. Florance. 2008. "Does Green Pay Off?" *The Journal of Real Estate Portfolio Management* 14 (4): 385–400.
- Ministry of Land, Infrastructure, Transport, and Tourism (MLIT) Japan. 2014. "Real Estate Appraisal Standards."
- Ono, E., S. Ito, and H. Yoshida. 2017. "Development of Test Procedure for the Evaluation of Building Energy Simulation Tools." *Proceedings of the International Building Performance Simulation Association* 380–388. doi:10.26868/25222708.2017.10z.
- Sanstad, A. H., and R. Howarth. 1994. "'Normal' Markets, Market Imperfections, and Energy Efficiency." *Energy Policy* 22 (10): 811–818. doi:10.1016/0301-4215(94)90139-2.
- Schleich, J. 2009. "Barriers to Energy Efficiency: A Comparison Across the German Commercial and Services Sector."

- Ecological Economics* 68 (7): 2150–2159. doi:10.1016/j.ecolecon.2009.02.008.
- SHASE. 2016. “SHASE-G 1008-2016, Guideline of Test Procedure for the Evaluation of Building Energy Simulation Tool.” Society of Heating, Air-Conditioning and Sanitary Engineers of Japan.
- Statistics Bureau of Japan (SBJ), Ministry of Internal Affairs and Communications. 2015. “Annual Report on the Labour Force Survey 2015.”
- Szumilo, N., and F. Fuerst. 2017. “Income Risk in Energy Efficient Office Buildings.” *Sustainable Cities and Society* 34: 309–320. doi:10.1016/j.scs.2017.06.024.
- Technical Committee on Electric Air Conditioning. 1992. “Heat Pump Air Conditioning System. Chapter 10, Economic Calculation.” Ohmsha, 978-4274101403.
- Togashi, E. 2015. “Effect of Energy Conservation Technology on Value of Real Estate. Part 2 Development of Stochastic Weather Process Model for Evaluate Risk of Energy Saving Investment.” *Transactions of SHASE Japan* 40 (223): 21–29. doi:10.18948/shase.40.221_21.
- Togashi, E. 2016. *The Art of Thermal Environmental Computing*. Togashi Lab. Kogakuin University. ISBN978-4990890810.
- Togashi, E. 2017. “Effect of Energy Conservation Technology on Value of Real Estate. Part 3 Development of Stochastic Office Worker Behaviour Model for Evaluating Risk of Energy Saving Investment.” *Transactions of SHASE Japan* 42 (240): 9–18. doi:10.18948/shase.42.240_9.
- Togashi, E. 2018a. “Effect of Energy Conservation Technology on Value of Real Estate. Part 4 Development of Stochastic Model of Tenant Characteristics.” *Transactions of SHASE Japan* 43 (253): 31–37.
- Togashi, E. 2018b. “Effect of Energy Conservation Technology on Value of Real Estate. Part 5 Quantification and Evaluation Method of Energy Saving Investment Risk Using Monte Carlo Method.” *Transactions of SHASE Japan* 43 (255): 21–28.
- Togashi, E., and S. Tanabe. 2009. “Methodology for Developing Heat-load Calculating Class Library with Immutable Interface.” *Technical Papers of the Annual Meeting of the Society of Heating, Air-conditioning and Sanitary Engineers of Japan: 1995–1998*. doi:10.18948/shasetaikai.2009.3.0_1995.
- Tuominen, P., and T. Seppänen. 2017. “Estimating the Value of Price Risk Reduction in Energy Efficiency Investments in Buildings.” *Energies* 10 (10): 1545. doi:10.3390/en10101545.
- Watanabe, T., Y. Urano, and T. Hayashi. 1983. “Procedures for Separating Direct and Diffuse Insolation on a Horizontal Surface and Prediction of Insolation on Tilted Surfaces.” *Transactions of the Architectural Institute of Japan* 330: 96–108.
- Wiley, J., J. Benefield, and K. H. Johnson. 2010. “Green Design and the Market for Commercial Office Space.” *The Journal of Real Estate Finance and Economics* 41 (2): 228–243.
- Yamagata, Y., D. Murakami, H. Seya, M. Tsutsumi, and Y. Kawaguchi. 2011. “An Analysis of Spatio-Temporal Effect of Green Building Rating on Real Estate Price.” *Journal of the Japanese Association of Real Estate Financial Engineering* 5: 23–39.
- Yoshida, H. 1992. “Modelling of Weather Data by Time Series Analysis for air-Conditioning Load Calculations.” *ASHRAE Transactions* 98: 328–345.